The Journal of Experimental Biology 216, 719-732

doi:10.1242/jeb.074732

RESEARCH ARTICLE

Visual motion speed determines a behavioral switch from forward flight to expansion avoidance in *Drosophila*

Michael B. Reiser[1,*] and Michael H. Dickinson[2]

[1]HHMI Janelia Farm Research Campus, 19700 Helix Drive, Ashburn, VA 20147, USA and [2]Department of Biology, University of Washington, Box 351800, Seattle, WA 98195-1800, USA

*Author for correspondence (reiserm@janelia.hhmi.org)

SUMMARY

As an animal translates through the world, its eyes will experience a radiating pattern of optic flow in which there is a focus of expansion directly in front and a focus of contraction behind. For flying fruit flies, recent experiments indicate that flies actively steer away from patterns of expansion. Whereas such a reflex makes sense for avoiding obstacles, it presents a paradox of sorts because an insect could not navigate stably through a visual scene unless it tolerated flight towards a focus of expansion during episodes of forward translation. One possible solution to this paradox is that a fly's behavior might change such that it steers away from strong expansion, but actively steers towards weak expansion. In this study, we use a tethered flight arena to investigate the influence of stimulus strength on the magnitude and direction of turning responses to visual expansion in flies. These experiments indicate that the expansion-avoidance behavior is speed dependent. At slower speeds of expansion, flies exhibit an attraction to the focus of expansion, whereas the behavior transforms to expansion avoidance at higher speeds. Open-loop experiments indicate that this inversion of the expansion-avoidance response depends on whether or not the head is fixed to the thorax. The inversion of the expansion-avoidance response with stimulus strength has a clear manifestation under closed-loop conditions. Flies will actively orient towards a focus of expansion at low temporal frequency but steer away from it at high temporal frequency. The change in the response with temporal frequency does not require motion stimuli directly in front or behind the fly. Animals in which the stimulus was presented within 120 deg sectors on each side consistently steered towards expansion at low temporal frequency and steered towards contraction at high temporal frequency. A simple model based on an array of Hassenstein–Reichardt type elementary movement detectors suggests that the inversion of the expansion-avoidance reflex can explain the spatial distribution of straight flight segments and collision-avoidance saccades when flies fly freely within an open circular arena.

Key words: elementary motion detector, insect vision, navigation, visual expansion.

Received 4 May 2012; Accepted 26 October 2012

INTRODUCTION

One essential feature of animal locomotion is the need to avoid obstacles. Organisms as different as paramecia (Kung, 1971) and humans (Lappe et al., 1999) possess specialized sensorimotor reflexes that enable them to detect objects in their path and make appropriate evasive maneuvers. One general challenge in the function of collision-avoidance reflexes is that they must operate with a sensitivity that balances the need for forward motion with the need to detect potential obstacles at a sufficient distance (Nelson and MacIver, 2006). For example, some animals use visual expansion cues to detect obstacles while moving, and respond to such signals when the predicted time-to-contact reaches a particular threshold (Wagner, 1982; Robertson and Reye, 1992; Wang and Frost, 1992; Hatsopoulos et al., 1995). Initiating an evasive maneuver at a higher threshold might not provide enough time or distance to avoid a deleterious collision, whereas triggering a response at a lower threshold might compromise forward progress through the environment. Presumably the control systems of animals have evolved to balance the needs of safety and locomotor efficiency.

Another intrinsic problem with collision-avoidance mechanisms based on optic flow is that forward locomotion creates a pattern of expansion that is similar to that of an approaching obstacle. In the fruit fly *Drosophila melanogaster*, the strength of expansion-avoidance reflexes are so strong that given a choice in a closed-loop tethered flight arena, flies will actively avoid a pole of expansion and actively steer towards a pole of contraction (Tammero et al., 2004). The strength of these turning reactions to expanding flow fields is substantially greater than those to rotatory flow fields at the same contrast and temporal frequency (Duistermars et al., 2007). These flight arena results present a paradox of sorts, because they suggest that flies stably prefer the pattern of optic flow created by backwards flight. Several subsequent studies have identified mechanisms that by diminishing the strength of the collision avoidance reflex, create a stable visual motor regime that permits prolonged sequences of forward flight. One such mechanism is that input to the antennae mimicking the head wind generated by forward locomotion modifies a fly's reaction to optic flow so that it is much more likely to steer towards a pole of expansion (Budick et al., 2007). In addition, tolerance of a forward pole of expansion is also increased by the presence of a salient visual target, such as a prominent vertical edge, suggesting that the expansion-avoidance reflexes are over-ridden in part by the presence of an attractive goal (Reiser and Dickinson, 2010).

Another explanation for the paradoxical avoidance of frontal expansion is that the reactions of the fly may depend on the strength of the visual stimulus. According to this hypothesis, the robustness of the collision-avoidance reactions measured in the past might be due to the strong stimulus conditions used to elicit them. Although not artifacts *per se*, such stimulus conditions might represent extreme conditions, mimicking, for example, what a fly might perceive immediately prior to collision. Presentation of a weaker expanding flow field, such as that generated by forward motion through an uncluttered landscape, might instead prove attractive to a fly. If this hypothesis is correct, then the sign of the animal's response should change with the strength of the stimulus. In a previous study we evaluated the collision-avoidance reflex under closed-loop behavior conditions over a range of contrast values (Reiser and Dickinson, 2010) and found no significant difference between reactions over the tested range. In this study we use a tethered flight arena to investigate the influence of the temporal frequency of expansion and the spatial extent of the expansion stimulus, on the magnitude and direction of collision-avoidance reflexes. These experiments have yielded novel insight – that the expansion-avoidance behavior exhibits a speed-dependent inversion. The results help to explain how the sensorimotor reflexes of animals are tuned to operate in both open and cluttered visual landscapes.

MATERIALS AND METHODS

Animal preparation and flight arena

Details of the fly preparation and visual display are identical to those described previously (Reiser and Dickinson, 2008). In brief, we used 3- to 4-day-old adult female *Drosophila melanogaster* from a laboratory culture originally derived from the interbreeding of the progeny of 200 wild-caught females. Flies were cold-anesthetized and tethered in a hover posture to a 0.1 mm tungsten rod. Flies were kept on a 12 h:12 h light:dark cycle, and were tested during the last 5 h of their subjective day. The cylindrical visual display was constructed from 44 LED panel modules for a resolution of 32×88 pixels, spanning ~94 deg of elevation and 330 deg in azimuth (Reiser and Dickinson, 2008). From the fly's vantage, the pixel sizes are non-uniform along the cylinder's elevation. The diameter of the largest pixel subtends a visual angle of 3.75 deg on the fly's retina, which is below the interommatidial distance of *Drosophila* (Heisenberg and Wolf, 1984). The luminance of 'on' pixels is 72 cd m^{-2}, and the maximum relative contrast of the display is ~93%, as measured using visual stimuli typical of the experiments described in this paper (Reiser and Dickinson, 2008). The wing positions were monitored via an optical sensor, called a 'wingbeat analyzer' (Götz, 1987; Lehmann and Dickinson, 1997), which provides instantaneous measurement of the wingstroke amplitude of both wings. The difference between these signals (ΔWBA) is taken as the animals' turning response. Data from the wingbeat analyzer and the visual display output signals were sampled at 500 Hz with a Digidata 1320A (Molecular Devices, Sunnyvale, CA, USA). All data analysis was performed offline using software written in MATLAB (MathWorks, Natick, MA, USA). In the statistical results presented we performed multiple comparisons correction by using the false discovery rate (FDR) controlling procedure (Benjamini and Hochberg, 1995).

Open-loop experiments

To explore the dependence of the collision avoidance reaction on stimulus strength, a series of open-loop experiments were conducted on head-fixed flies, in which a small amount of UV-activated glue was used to bind the back of the head to the thorax, as well as with head-free flies, in which the thorax was fixed to the tethering pin, but the head was free to rotate. The data presented in Fig. 1 correspond to head-fixed flies, and all other results are from head-free animals. All experiments involved a manipulation of the basic expansion/contraction pattern described previously (Reiser and Dickinson, 2010). This pattern is a simple approximation of the optic flow field that an animal would experience if it translates through a cluttered environment without rotating (Helmholtz and Southall, 1925; Gibson, 1950). Under these conditions, a moving agent experiences a visual focus of expansion (FOE) in the direction of motion and, if vision were panoramic, a focus of contraction (FOC) directly behind. The exact pattern depends critically on the spatial distribution of objects in the environment, but in our case we followed the approximation of previous experimenters (Tammero et al., 2004; Duistermars et al., 2007) by representing the flow field as regular gratings that emerge from the FOE and converge at the FOC. The standard grating pattern consisted of 4-pixel-wide vertical bars of active and inactive pixels for a spatial period (λ) of 8 pixels, or 30 deg cycle^{-1}. We use the term 'spatial frequency' as a rough proxy describing only the fundamental frequency of the square wave pattern. This spatial frequency is in the range that evokes near-maximum optomotor reactions in *Drosophila* (Buchner, 1976). The absolute azimuthal position of the FOE and FOC is set experimentally in open-loop or controlled by the fly in closed-loop *via* feedback from the wingbeat analyzer. The primary manipulations of the pattern in this study relate to changes in the rate of the expansion component of the stimulus, which we quantify using the pattern's temporal frequency (f_t).

The open-loop, head-fixed fly experimental series contained six expansion rates (temporal frequency of 0.25, 0.5, 1, 2, 4 and 8 Hz), with the FOE located at eight positions around the fly (0, ±45, ±90, ±135 and 180 deg), presented in random block trials. In Fig. 1B,C the 4 Hz condition is omitted for clarity. This experiment made use of a simplified, non-dithered (see below), expansion-rotation pattern in which the edge transitions were immediate, but the basic results have been verified with the identical pattern as used in Fig. 2 (data not shown). The experimental series consisted of a 4 s test phase of open-loop expansion, followed by 5 s of closed-loop stripe fixation, in which the fly controls the angular velocity of a 30 deg dark stripe by adjusting the bilateral difference in stroke amplitude (ΔWBA). To quantify the flies' turning responses, we calculated the mean ΔWBA value during the 4 s epoch of pattern motion. For each trial, the mean response during the 100 ms period immediately preceding stimulus presentation was subtracted from the subsequent response. Before combining data across flies, the mean turning response for each fly was determined first using a normalization procedure described previously (Reiser and Dickinson, 2010), which averages (in a sign conserving manner) an individual fly's responses to bilaterally symmetrical presentations of each stimulus. Data from flies that stopped flying before completing at least two full blocks of trials were discarded. In total, 23 flies completed between two and three repetitions of this 7.2 min protocol.

During the open-loop, head-free experiments we tested five expansion rates (temporal frequencies of 0.125, 0.25, 0.5, 1 and 8 Hz), with the FOE located at 10 different positions around the fly (0, ±30, ±60, ±90, ±135 and 180 deg). These conditions were selected to more densely sample the slower speeds of expansion for FOE positions near the front where we observe a speed-dependent inversion of the behavioral response. For all of the rates of expansion except the fastest (8 Hz), we use the display's intermediate intensity values to achieve smoother stimulation by dithering the pattern (Reiser and Dickinson, 2008). With this configuration, a dark edge

turns bright gradually via four intermediate intensity values, taking 24 frames (rather than eight) to progress through one cycle of the grating. The experimental series consisted of a 4 s test phase of open-loop expansion, followed by a 5 s trial of a closed-loop fixation. The 50 stimulus conditions were presented in random block trials. Only data from flies that completed at least two repetitions of this protocol were used for analysis. In total, 36 flies completed between two and three repetitions of this 7.5 min protocol, with the results presented in Fig. 2.

Closed-loop experiments

A closed-loop assay allows the fly to actively control the azimuthal orientation of the 'translational' pattern by adjusting the bilateral difference in their wing stroke amplitude. In these experiments the temporal frequency of the drifting square wave pattern was fixed (open-loop) to the desired experimental value. However, a signal proportional to the difference in wing stroke amplitude was used to adjust the angular velocity with which the whole pattern of translational flow rotated around the animal. Under such conditions, the fly could choose to orient towards (or 'fixate') any angular position within the flow field, including the FOC or FOE. A more detailed description of this experimental protocol and data analysis has been described (Reiser and Dickinson, 2010). Consistent fixation of the FOC was rarely exhibited by head-fixed flies, and so for the closed-loop experiments we used head-free animals [the study that initially reported the fixation of the FOC (Tammero et al., 2004) also made use of head-free animals].

An important objective of the experiments was to minimize any *a priori* determination of the most behaviorally appropriate stimulus conditions, so a large set of spatial and temporal frequencies of the expansion motion were tested. Patterns of three spatial periods (λ=15, 30 and 60 deg) were created, and moved at six different angular velocities (the temporal frequency is the ratio of the angular velocity and the spatial period of the pattern), yielding 18 experimental conditions. Each closed-loop trial was 40 s since this was the shortest period of time determined to adequately capture the behavioral preference of the animals with limited influence of the initial conditions. The experimental series also contained one trial for each pattern that was 'expanded' at 0 frames s^{-1}, a condition that generates a pure rotatory optomotor stimulus (these data are not shown). These trials were interspersed with 5 s of closed-loop stripe fixation in random blocks. In total, 16 flies in the data set completed between one and two repetitions of 15.75 min protocol. Data from flies that failed to complete at least one full block of trials were discarded. The results of these experiments are presented in Fig. 4.

Controls for simplistic geometry of optic flow patterns

One possible explanation for the strong expansion-avoidance behaviors observed in flight arena experiments (Tammero et al., 2004) is that the response could be an artifact of the simple cylindrical pattern, which provides too crude an approximation of typical optic flow patterns perceived during free flight. In particular, the patterns of expansion and contraction (directly in front of and behind the fly, respectively) in our standard translational pattern are stronger, relative to the lateral flow fields, than what might be experienced by an animal flying within a visually sparse environment or through the center of a long tunnel. To test the possibility that our results might be biased by the specific reactions to expansion or contraction in the front and rear visual fields, we examined the closed-loop expansion-avoidance behavior under conditions in which the spatial extent of the pattern was restricted. The patterns used were based on a square wave grating (λ=30 deg) with the smoother, dithered edge transitions described above. To display motion restricted to the lateral portions of the arena, two patterns were designed with all pixels in the front and rear sectors of the arena set to a static intermediate intensity (3/7 the brightness of the 'on' pixels in our grating pattern). These experiments were performed at three temporal frequencies of expansion and consisted of 40 s closed-loop trials, during which one of three patterns (180, 120 and 60 deg extent per side) was presented at one of the three temporal frequencies of expansion (0.25, 0.625 and 5 Hz). These trials were interspersed with 5 s of closed-loop stripe fixation (during which we present the complete, unrestricted pattern), in random block trials. In total, 13 flies (head-free) completed between two and three repetitions of this 6.75 min protocol. Data from flies that failed to complete at least one full block of trials before stopping were discarded. The results of these experiments are presented in Fig. 5.

Simulation of fly motion vision and free-flight behavior

The motion detection system of flies (Borst and Egelhaaf, 1989), is well approximated by simple compound eye optics above luminance collectors that feed an array of Hassenstein–Reichardt elementary motion detectors (HR EMDs) (Hassenstein and Reichardt, 1956; Reichardt, 1961). Because the experiments discussed here rely on rotational responses of the animal to motion presented on a cylindrical display, we model a simplified, planar retina, representing an equatorial cross-section through the fly's eye. In *Drosophila*, the ommatidial array is distributed with near uniformity throughout the eye, with an overlap of ~5–10 deg in the front, and a blind spot of roughly 40 deg directly behind (Büchner, 1974; Heisenberg and Wolf, 1984). A schematic of our simulated fly eye is shown in Fig. 6A. The basic HR EMD implements the 'delay and correlate' algorithm with the inputs to each paired motion detector being signals from adjacent ommatidia (Buchner, 1976). We simulate the point-spread function of the ommatidial lens (which acts as a spatial low-pass filter), $L(\Theta)$, as a Gaussian sampling function of the form:

$$L(\Theta) = k\exp\left[-\frac{4\ln 2}{\Delta\rho^2}\Theta^2\right], \quad (1)$$

where k is the normalization constant, $\Delta\rho$ is the acceptance angle of an ommatidium and Θ is the vector of positions around the eye. This fit for the compound eye optics is based on Snyder (Snyder, 1979), with the notation of Burton and Laughlin (Burton and Laughlin, 2003). In the simulations of the *Drosophila* eye, we use $\Delta\rho$=5 deg after Buchner (Buchner, 1984). The circular retina is modeled as an array of 72 such ommatidia, with a binocular overlap of one ommatidium in the front and a blind spot of ~20 deg per side in the rear. Buchner (Buchner, 1984) specified that the interommatidial angle for *Drosophila* is 4.6 deg; to simplify the simulation we use 4.5 deg. The retinal image is formed by the convolution of the intensity signal $I(\Theta,n)$, a function of angular position and the discrete sample time, n, with the acceptance function of the photoreceptors: $R(n)=L(\Theta)*I(\Theta,n)$. The retinal image $R_j(n)$, where j is the index of ommatidia, is obtained by matrix multiplication. This simulation does not implement the details of neural superposition, and so the 'photoreceptor' captures all light sampled through one ommatidium.

Ray casting is used to simulate the view of the equator of the fly eye within a virtual, cylindrical arena. At each simulation time step, the intersection of the rays emanating from the sampled

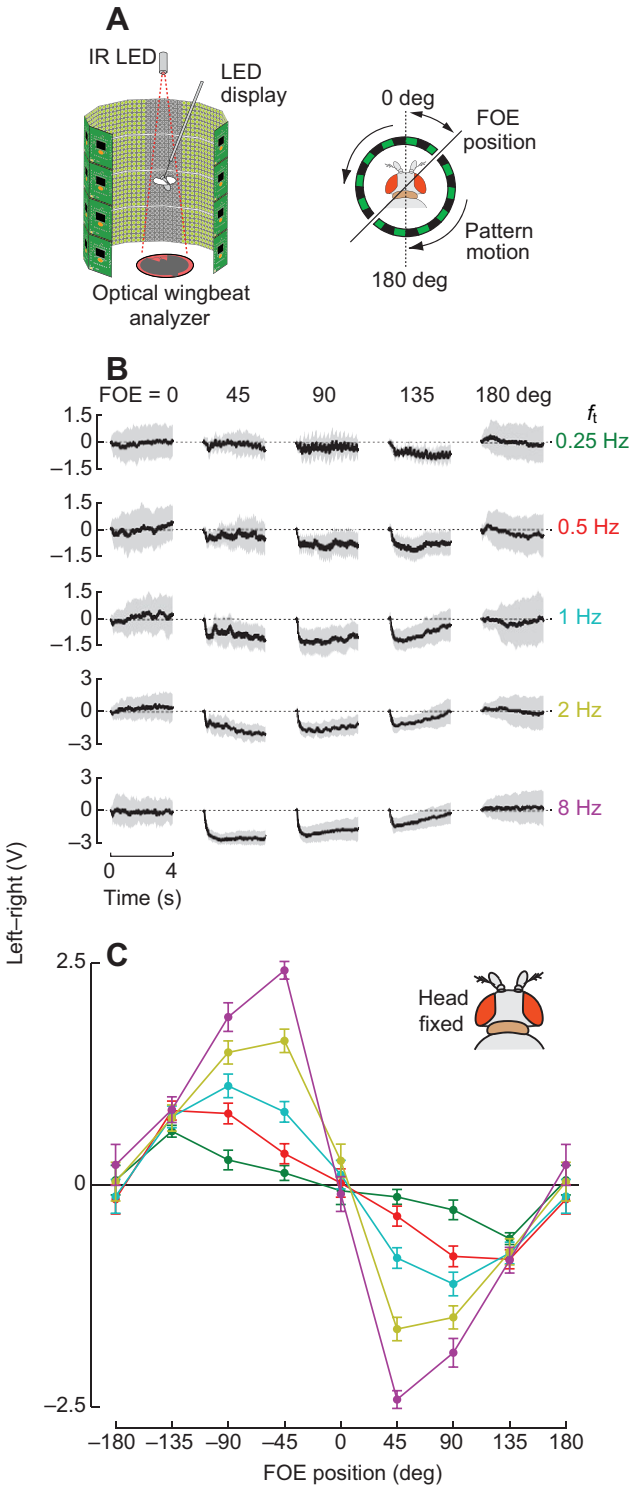

Fig. 1. The steering response of head-fixed *Drosophila* to large-field expansion. (A) A schematic of the experimental apparatus, in which a fly is positioned above an optical wingbeat detector, in the center of a cylindrical LED display. In these experiments the heads of the flies have been immobilized by gluing. An expansion pattern, composed of gratings that emanate from the focus of expansion (FOE), is presented to flies from different positions around the circumference of the arena. (B) The mean ± s.d. turning responses (difference between left and right wingstroke amplitudes) of flies to expansion patterns emanating from five azimuthal positions (mirror symmetric presentation on the left of the animal have been averaged with the presented data), at five temporal frequencies (f_t), are shown; N=23 flies. The responses to the slower speeds show phase-locking to the advances of the expansion pattern, and the turning responses to the f_t=2 Hz stimulus show phase-locking to the temporal frequency of the stimulus pattern. The turning responses are integrated and plotted as a tuning curve (C). The mean ± s.e.m. turning response shows that flies turn away from the FOE at all speeds, except for the responses to frontal and rear expansion, which are on average close to zero.

positions of Θ is determined by line–circle intersection, which are then compared with the pattern to determine the intensity signal, $I(\Theta,n)$. The identical simulation was implemented for the tethered fly experiments within the flight arena, and is used for Fig. 6B,C.

The array of Hassenstein–Reichardt motion detectors is used to compute the optic flow field from $R_j(n)$. A first-order low-pass filter (time constant τ) is used to accomplish the delayed intensity signal required for the EMD computation. The temporal frequency optimum (TFO) of the HR EMD is entirely determined by τ (TFO=1/2πτ). We use τ=30 ms, which yields TFO=5.3 Hz, in agreement with the TFO of the expansion-avoidance behavior in Fig. 4. We define two digital filter coefficients, A=1–2τ/h and B=1+2τ/h, where h is the temporal sampling interval, 1 ms in our simulation. The delayed intensity function at each retinal position is:

$$D_j(n+1) = [R_j(n+1) + R_j(n) - A \times D_j(n)] / B. \quad (2)$$

Finally, the response of the HR EMD array is computed by multiplying the delayed signal at each position by the current value at the neighboring position and subtracting the resulting value of the mirror symmetric pair. The right and left halves of the retina are treated as separate inputs. The responses of the motion detector array are computed as:

$$ML_k(n) = D_k(n) \times R_{k+1}(n) - D_{k+1}(n) \times R_k(n), \quad (3)$$

$$MR_k(n) = D_{k+36}(n) \times R_{k+37}(n) - D_{k+37}(n) \times R_{k+36}(n), \quad (4)$$

where k indexes the motion detector array output from the right and left eye. The motion detector outputs are then filtered with a first-order low-pass filter with τ_o=200 ms, established to account for sensorimotor delays.

RESULTS

Effect of temporal frequency on open-loop expansion avoidance

The study that established the expansion-avoidance behavior in *Drosophila* (Tammero et al., 2004) showed rather convincingly that flies avoid the FOE of an expanding pattern. Specifically, that study examined the open-loop steering responses of flies to full-field expansion/contraction patterns of optic flow emanating from different azimuthal positions (Tammero et al., 2004). The results indicate that animals steer away from the FOE and towards the FOC, a reaction polarity that is consistent with a collision-avoidance response. The first goal of this present study was to examine how the magnitude and sign of this reflex might change in response to weaker expansion stimuli, and we set out to test this by varying the temporal frequency of the expanding pattern.

To more accurately map the spatial sensitivity of this behavior, we chose to stabilize the image presented to the flies by testing head-fixed *Drosophila*. To gauge the turning behavior of the flies in response to the stimuli, we used the mean left minus right

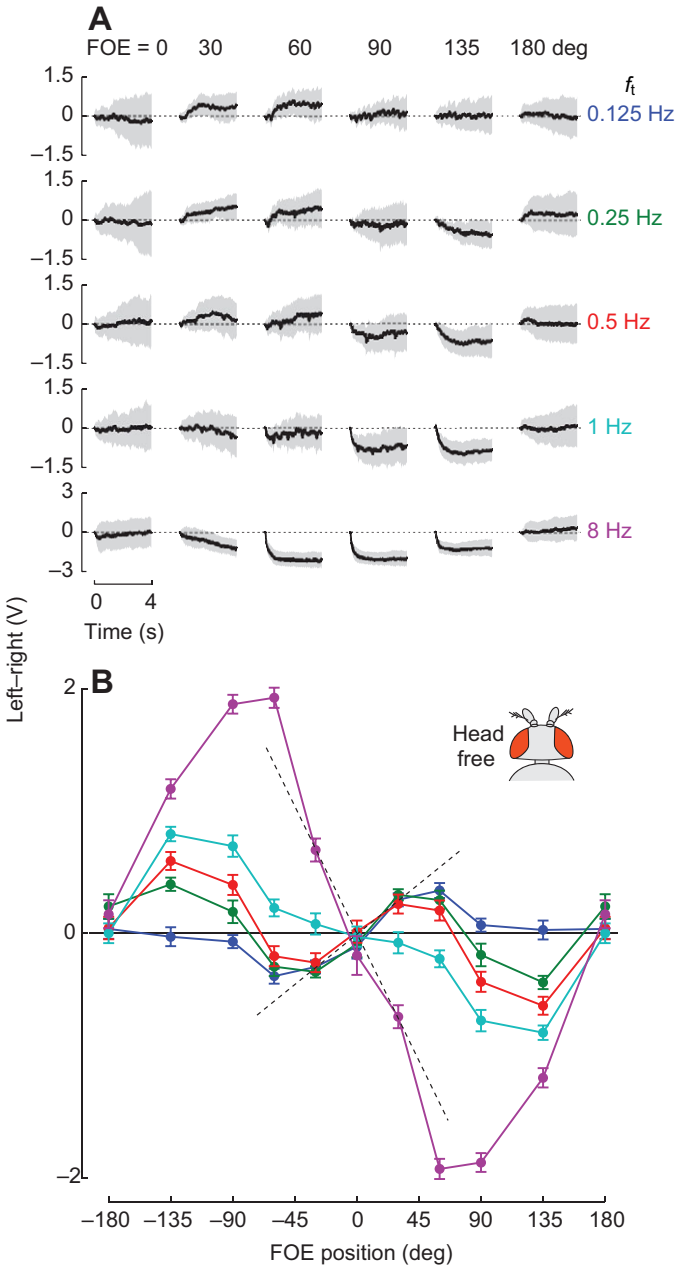

Fig. 2. The steering response of head-free *Drosophila* to large-field expansion depends on the speed of visual motion. The experiments presented in Fig. 1 were repeated in head-free flies and the stimuli were selected to prioritize slower expansion speeds presented near the front of the animals. The plotting conventions are the same as in Fig. 1. (A) The mean ± s.d. turning responses to the expansion emanating from six azimuthal positions, at five temporal frequencies, are shown; N=36 flies. The responses to the three slower speeds show phase-locking to the advances of the expansion pattern, most noticeable for the lateral FOE positions. The turning responses are integrated and plotted as a tuning curve (B). The mean ± s.e.m. turning response shows that flies turn away from expansion at all speeds when it is positioned laterally and rearward. However, at lower rates of expansion, the turning direction is opposite – the flies turn so as to orient towards the FOE. The dashed lines are drawn to emphasize that the slope of the response curve near the origin to expansion of different speeds changes sign, predicting that the FOE should be frontally stable at slower speeds, but unstable at the higher rates of expansion. The turning response shows that permitting head movement in tethered flies uncovers an orientation behavior that could be used to guide forward flight.

wingbeat amplitude during the short periods of pattern motion (Fig. 1A). These mean speed- and position-dependent turning responses (with an envelope indicating standard deviation) are shown as time series in Fig. 1B, in which each column indicates the responses to the FOE at a given azimuthal position, and each row indicates the responses at a given temporal frequency. For each, the mean turning response was determined by first combining the data for the symmetric presentations of motion (after an inspection to ensure that the data were indeed nearly symmetric).

As reported earlier (Reiser and Dickinson, 2010), the time series traces show a repetitive jitter at the lowest temporal frequency (f_t=0.25 Hz), which is evidence that the motor system is phase-locked to the discrete pattern advances of the expansion stimulus under these conditions. At higher temporal frequencies, a second type of ripple is observed, which corresponds to phase-locking to the temporal frequency cycles of the pattern (most noticeable at f_t=2 Hz, where indeed the entrainment is to the 2 Hz stimulus). Across speeds, the reactions to a frontal (0 deg) or rear (180 deg) FOE are approximately zero and turns in response to all other positions of the FOE are away from the FOE. For example, the reactions to the FOE at 90 deg are all negative, corresponding to a clockwise torque that would result in rotating the FOE rearward.

The FOE avoidance reactions are most clearly visualized as a directional tuning curve (Fig. 1C). Across all speeds, the tuning curve resembles those described previously by Tammero et al. (Tammero et al., 2004), and exhibits an inverse sine shape that is consistent with a collision-avoidance reaction in which the animal would always steer away from the FOE. For all speeds, the distributions of reactions to a frontal (0 deg) or rear (180 deg) FOE are not significantly different from zero (t-test, FDR controlled with q=0.05) and all mean turn distributions for FOE positions other than frontal and rear are significantly different from zero, except for the reaction to the FOE at ±45 deg and f_t=0.25 Hz condition (t-test, FDR controlled with q=0.05). The result that flies turn away from the FOE holds even at the lowest speed tested (f_t=0.25 Hz), although the curve is markedly less sinusoidal in this case. At all tested expansion rates, however, the average turning response exhibited to lateral positions of the FOE is unambiguously away from the position of the FOE.

While testing head-fixed flies in the aforementioned experiments, we noticed that these flies did not exhibit the very robust orientation for the FOC under closed-loop condition that was reported in Tammero et al. (Tammero et al., 2004). We did confirm, however, that tethered, head-free flies did produce the reported closed-loop behavior – a result that is consistent with the fact that the prior study used head-free flies. This difference in the behavior of head-free and head-fixed flies under closed-loop conditions motivated us to conduct a pilot study of the open-loop behavior of head-free flies, using the protocol of Fig. 1 (results not shown), and based on those findings, we conducted more extensive experiments after adapting the protocol to more finely sample the slow speeds and frontal locations of the FOE.

The mean turning responses (with an envelope indicating standard deviation) are shown as time series in Fig. 2A, using the same plotting conventions as in Fig. 1. These time series show several interesting features. As was the case for the head-fixed results, we again see phase-locking to the discrete pattern advances of the expansion stimulus. This phase-locking can clearly be seen in the mean response to the f_t=0.125 Hz expansion (updated at three frames per second), and is also present in the responses to the f_t=0.25 Hz and f_t=0.5 Hz expansion, but is not seen in the responses to faster rates. The presence of this ripple has been used to determine an

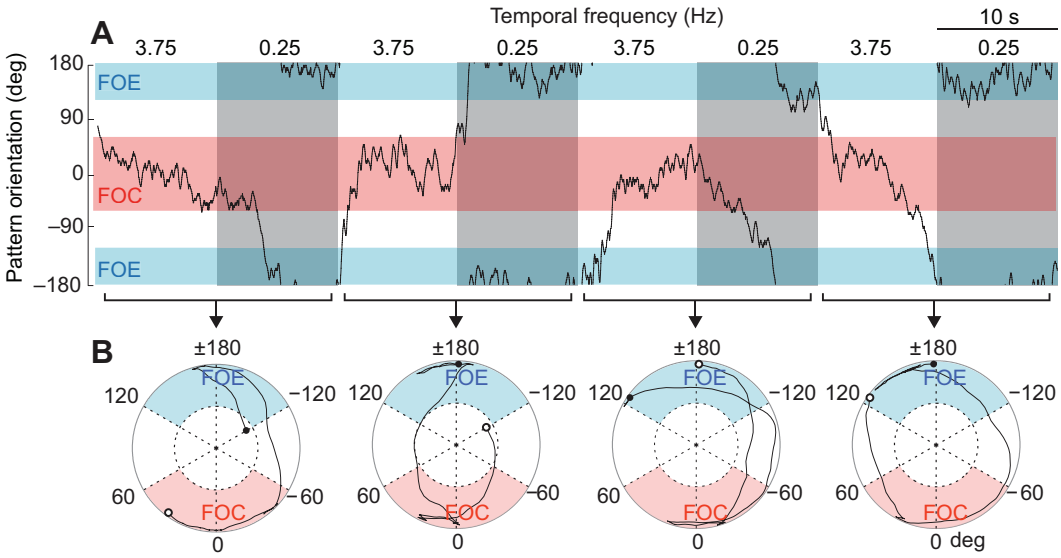

Fig. 3. The orientation preference of *Drosophila* flying under closed-loop expansion-avoidance can be quickly altered by changing the rate of pattern expansion. The example orientation behavior of an individual (head-free) fly is shown, while the temporal frequency is alternated every 10 s from a faster temporal frequency of 3.75 Hz, to a slower one of 0.25 Hz (denoted by the gray bars). The red rectangle outlines the orientation of the pattern that we quantify as focus of contraction (FOC) orientation, and the blue rectangles (top and bottom) indicate the bounds we apply to FOE orientation. As predicted by the open-loop turning responses shown in Fig. 2, this closed-loop orientation behavior demonstrates that flies orient towards the FOC at high speeds and at lower speeds the FOE is actively preferred. To better quantify the orientation preference of flies, a moving 2 s window of the circular mean and the mean resultant length, *r*, were computed. To display this transformation we plot these as trajectories in polar coordinates, for four 20 s segments (open circles mark the beginning of each trajectory and closed circles indicate the end). If $r>0.5$, then the pattern position is treated as stable, and if either the FOC (area shaded red) or the FOE (shaded blue) is frontal, then that time window is assigned accordingly.

appropriate 'visuomotor' time constant in the simulation results that follow. The larger downward deflections that can be seen in the average traces of the f_t=0.25, 0.5 and 1 Hz stimuli correspond to a response to a 'new' bar which occurs at the rate governed by the temporal frequency of the pattern. The majority of these time series curves (ignoring the modest fluctuations just described) qualitatively resemble the step response of a low pass filtered system that has reached (on average) its steady-state level by 1 s of the 4 s trial. However, there are some exceptional conditions, such as the responses to the 8 Hz expansion stimulus with the FOE at the ±30 deg position, which show very slow accumulation of the response, suggesting that somehow the position of the FOE influences the temporal dynamics of the expansion-avoidance reaction.

The most substantive difference between these responses and the head-fixed data in Fig. 1 is the emergence of a temporal frequency-dependent reversal of the steering responses. This can be directly seen by comparing the polarity of the responses in the top (lowest f_t) and bottom (highest f_t) rows, for the ±30 deg and ±60 deg conditions. The responses to the two highest speeds tested (f_t=1, 8 Hz) look very much like the results from Fig. 1, whereas at slower speed the responses exhibit an inversion that is position dependent. For example, the reaction to f_t=0.5 Hz changes sign across the third row of Fig. 2A, indicating that the response to the frontal FOE positions is a turn towards the FOE, whereas the response to lateral and rearward FOE positions is a turn away from the FOE. This speed- and position-dependent inversion is clearly seen in the directional tuning curve in Fig. 2B. Across speeds, the distributions of reactions to a frontal (0 deg) or rear (180 deg) FOE are not significantly different from zero (*t*-test, FDR controlled with q=0.05). All other turning reactions to the remaining FOE positions are significantly different from zero, with the exception of these conditions: FOE at ±90 deg and ±135 deg for f_t=0.25 Hz, FOE at ±90 deg for f_t=0.25 Hz, and FOE at ±30 deg for f_t=1 Hz (*t*-test, FDR controlled with q=0.05). At temporal frequencies above 1 Hz, the tuning curve resembles that described previously (Tammero et al., 2004), and exhibits an inverse sine shape that is consistent with a collision-avoidance reaction in which the animal would always steer away from the FOE. At speeds below 1 Hz, however, the tuning curve is distorted and resembles a non-inverted sine wave at double frequency. The dashed lines superimposed on the tuning curves are presented to emphasize the inversion in the slope of the steering reaction to small deviations in the position of a frontal FOE. At high speeds a negative response slope indicates a turn away from the FOE, whereas at slow expansion speeds the positive sign of the slope indicates that flies would steer towards the FOE. Under our testing conditions, the critical temporal frequency defining the transition between FOE attraction and FOE avoidance occurs between 0.5 and 1 Hz, where the reaction to 1 Hz expansion appears to be just above this threshold. Taken together, the results in Fig. 2 reveal that the strong preference for orienting towards the FOC is reduced only at low temporal frequencies and for locations near the front of the visual field. Furthermore this inversion of the turning reaction can only be observed in head-free flies.

Temporal frequency dependence of closed-loop expansion avoidance

To further test whether the speed-dependent inversion of the aversive reaction to a FOE could be related to the forward flight paradox, we performed a set of closed-loop experiments in which the fly could actively steer towards any position in the pattern by adjusting its stroke amplitude difference. The open-loop responses in Fig. 2 suggest that flies will selectively orient towards the FOE at slow speeds and the FOC at higher speeds. A direct test of this prediction is shown Fig. 3A, which plots a fly's closed-loop

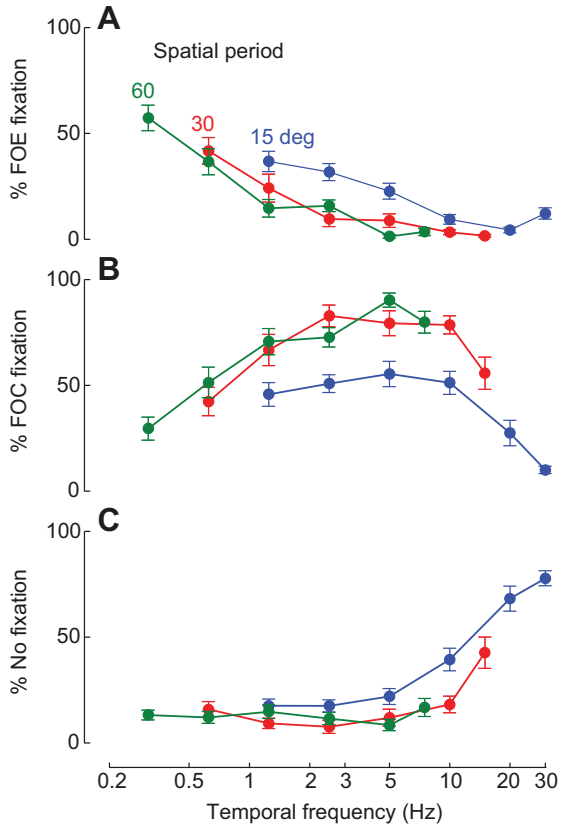

Fig. 4. Flies exhibit a strong preference for orienting towards expansion at low temporal frequencies. The percentage of time that flies spend orienting towards the FOE (A), the FOC (B) or neither (C) is shown, as determined by the orientation scoring procedure (Fig. 3). The mean ± s.e.m. scores for the 18 tested combinations of spatial period (15 deg in blue, 30 deg in red and 60 deg in green) and frame rate, are plotted on a log scale of temporal frequency; N=16 flies. These data show that at low temporal frequencies, flies prefer orienting towards the FOE, but prefer orienting towards the FOC for faster conditions. For all spatial periods, FOC fixation is most prominent around f_t=5 Hz and decays at higher and lower temporal frequencies.

orientation response while the temporal frequency of the expanding/contracting pattern was switched from 3.75 to 0.25 Hz every 10 s. The trace largely supports the predictions, in that the fly's behavior alternates rapidly from FOC fixation (within the red-outlined horizontal band) at the fast temporal frequency to FOE fixation (within the blue-outlined horizontal bands) at the lower temporal frequency. However, this example also shows that the fly can exhibit transient fixation of either the FOC or FOE, especially in the first few moments after a change in temporal frequency. To facilitate the further analysis of such data, we make use of a previously described technique (Maimon et al., 2008; Reiser and Dickinson, 2010) that converts these data into a polar coordinate representation of the mean orientation angle and the mean resultant length, r, during a 2 s sliding window. The magnitude of r lies between 0 and 1 and is related to the dispersion of the data about the mean orientation (the circular variance is $1 - r$, so when r=0, variance is maximal and when r=1, variance is 0). The transformed version of the example sequence is shown in Fig. 3B, which highlights the bouts of FOE and FOC orientation and the transitions between them. Using this scheme, it is possible to classify the flies' orientation behavior: epochs within the red region are classified as 'FOC fixation', those within the blue sector as 'FOE fixation', and data within the white region are classified as 'no fixation'.

To investigate this speed-dependent orientation preference more systematically, we examined the closed-loop behavior of flies using several spatial periods and expansion rates. We varied the spatial period of the pattern to examine the robustness of the speed-dependent inversion and to determine whether the behavior exhibited properties that are consistent with the canonical model for fly motion detection, the Hassenstein–Reichardt elementary motion detector (HR EMD). The orientation preference is quantified as the percentage of time spent orienting towards the FOC, the FOE, or neither, and is shown in Fig. 4 as a function of the temporal frequency of the pattern with a separate curve for each spatial period. The data show that at lower temporal frequencies the flies selectively orient towards the FOE, whereas the robust FOC fixation that has previously been described (Tammero et al., 2004) only occurs at higher temporal frequencies. At the lowest f_t tested, λ=60 deg and f_t=0.3125 Hz, the preference for orienting towards the FOE is significantly higher than for orienting towards the FOC, whereas at the two conditions with the next lowest speed, f_t=0.625 Hz with λ=30 deg and λ=60 deg, the flies appear to exhibit a bistable preference as there is no significant preference between the time spent orienting towards the FOE *versus* the FOC (Mann–Whitney U-test, FDR controlled with q=0.05). At higher temporal frequencies, the turning preference for the FOC is significantly greater than for the FOE for all tested conditions, except for two speeds of the λ=15 deg stimulus: f_t=1.25 Hz, where the FOC and FOE are again equally preferred, and f_t=30 Hz, where the preference for either focus is greatly attenuated (U-test, FDR controlled with q=0.05). For all spatial periods, FOC fixation is most prominent at 5 Hz and decays at higher and lower temporal frequencies. The behavior of the flies did not change substantially for the tested spatial periods, and are nearly identical for the λ=30 deg and λ=60 deg conditions (i.e. the percentage of FOC orientation is not significantly different at the four temporal frequencies where both spatial periods were tested; U-test, FDR controlled with q=0.05). However, the closed-loop orientation behavior for the λ=15 deg pattern shows reduced fixation. This effect was largely due to a higher percentage of time during which the pattern was rapidly spinning (Maimon et al., 2008), which in our scheme was classified as 'no fixation'. In agreement with the open-loop results in Fig. 2, the FOE is most attractive during conditions with temporal frequencies below 1 Hz, although significant FOE orientation is seen in the λ=15 deg conditions for temporal frequencies up to 10 Hz.

Closed-loop expansion avoidance with restricted spatial extent

To what extent does the speed-dependent inversion require the complete, idealized expansion pattern we have presented thus far? To better approximate the patterns seen by, for example, a fly flying down a corridor, we modified the patterns so that the grating motion was present only in the lateral fields of view. Flies were given active control over the rotational velocity (and thus the position of the FOE/FOC) of the expanding/contracting flow pattern drifting at one of three temporal frequencies, with either a 180, 120 or 60 deg azimuthal sector visible per side. The forward and rear sectors in which no stimulus motion occurred were filled with a static pattern of intermediate intensity, producing a masked version of the expansion/contraction pattern used for the experiments of Figs 3 and 4. The resulting orientation behavior is summarized as polar histograms in Fig. 5A, and further quantified as the percentage of time that flies spent fixating the FOE and FOC in each trial (mean

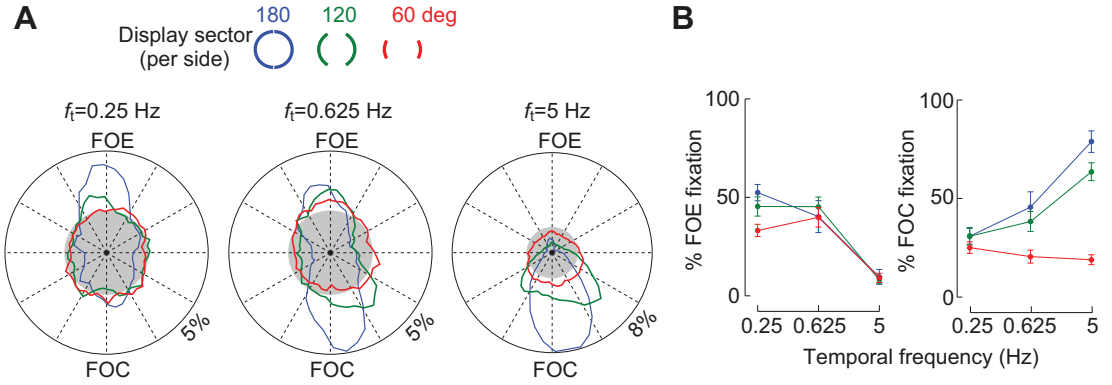

Fig. 5. The change in the response with temporal frequency does not require motion stimuli directly in front of or behind the fly. To examine the dependence of the expansion-avoidance behavior on the global expansion pattern, we tested laterally restricted motion patterns. The orientation histograms (A), grouped by the temporal frequency of expansion, are plotted with orientation towards the FOE at the top of the polar plot; N=13 flies. The gray circles indicate the distribution associated with uniform orientation. The fixation scores (B) show the mean ± s.e.m. percentage of time that flies spend orienting towards the FOE and FOC, respectively. At each temporal frequency tested, the orientation behavior observed for the complete pattern is largely unchanged for the stimuli restricted to 120 deg side sectors. When further reduced to 60 deg side sectors, there is little further reduction in the FOE orientation, while the FOC orientation at f_t=5 Hz is abolished.

± s.e.m. orientation scores are plotted in Fig. 5B; the redundant 'no fixation' category is omitted). The histograms corresponding to complete azimuthal coverage (blue traces) as well as the summary measures of fixation percentage agree with the previous results; FOE orientation is significantly preferred at f_t=0.25 Hz, the behavior at f_t=0.625 Hz shows orientation towards both foci with no significant preference, and the behavior at f_t=5 Hz is significantly dominated by FOC orientation (U-test, FDR controlled with q=0.05). The data also suggest that the dependence of the orientation behavior on temporal frequency is largely unchanged when the stimulus pattern was restricted to 120 deg side sectors (green traces; i.e. the flies selectively orient towards the FOE at f_t=0.25 Hz and the FOC at f_t=5 Hz). The data in the polar histograms indicate that the orientation tuning is not as precise when the front and rear 60 deg sectors are masked (comparing blue and green data), but just such a degradation in tuning is expected because when there is no stimulus visible in front of the fly, the location of the foci of the pattern must rotate beyond the masked zone before the fly can respond. Nevertheless, the orientation preference (Fig. 5B) towards the FOE is not significantly different for these two patterns at the three temporal frequencies tested, while the orientation percentage towards the FOC is only significantly different for f_t=5 Hz (U-test, FDR controlled with q=0.05). The results from the trials in which the pattern was restricted to 60 deg side sectors (red traces) show a prominent difference with the results from the more complete pattern conditions. At f_t=0.25 Hz, the flies show a small, but significant decrement in the fixation towards the FOE (U-test, FDR controlled with q=0.05), as is expected by the further reduction in spatial information about the location of the foci. Furthermore, the flies exhibited a reduction in FOE fixation at high temporal frequency, as in the 180 and 120 deg cases (Fig. 5B, left, where the FOE fixation percentages for the three patterns at both higher speeds are not significantly different; U-test, FDR controlled with q=0.05), but in contrast the flies did not show a concomitant increase in FOC fixation (Fig. 5B, right). In the intermediate case of f_t=0.625 Hz, the orientation towards the FOE is consistent with the level exhibited in the 180 and 120 deg cases, but FOC fixation is reduced (Fig. 5B, right, orientation towards the FOC for the 60 deg lateral pattern is significantly lower than for the other two patterns at the two highest speeds; U-test, FDR controlled with q=0.05). This inability to orient towards the FOC during conditions of fast expansion when the forward and rear visual fields are severely restricted suggests that orientation towards the FOC, but not the FOE, depends on the analysis of optic flow in front of, and possibly behind, the animal. This finding may provide further clarification on the forward flight paradox. When the strong, rather artificial optic flow at the foci of the expansion/contraction pattern is masked, the paradoxical orientation towards the FOC is reduced, whereas flight towards the FOE that is prominent at the lower expansion rates is maintained.

Collectively, the closed-loop experiments indicate that a fly's active orientation behavior within a simple translation optic flow pattern is strongly influenced by the temporal frequency of the drifting pattern. Gentle, low temporal frequency expansion conditions promote fixation of the FOE, whereas strong, fast expansion stimuli promote fixation of the FOC. Furthermore, the lack of dependency on spatial period suggests a process mediated by HR EMDs. In addition, fixation of the FOC (and thus avoidance of expansion) appears to require that strong stimulus cues are visible over large portions of the visual field, especially the front and possibly rear visual sectors. Based on these results, as well as those derived from the open loop experiments of Figs 1 and 2, we now present a model of how a temporal frequency dependence of fixation behavior could lead to vision-based flight control scheme that balances the need for forward progress with obstacle avoidance.

Simulation of expansion avoidance behavior

Does the critical temporal frequency governing the speed-dependent switch from orientation towards to avoidance of the FOE occur within a range of behaviorally relevant visual conditions? This question cannot be directly answered because the speed of visual motion encountered by flying flies is tightly regulated based on the available visual conditions (David, 1982; Franceschini et al., 2007; Fry et al., 2009). Therefore we chose to make use of existing experimental results to constrain a simulation of *Drosophila* free flight behavior.

We implemented a simulation of an array of HR EMDs, which receives input from photoreceptors with optics modeled after the *Drosophila* compound eye (Fig. 6A). The response of the modeled EMD to the motion of patterns with the three spatial periods used in the experiments of Fig. 4 (and a larger range of temporal

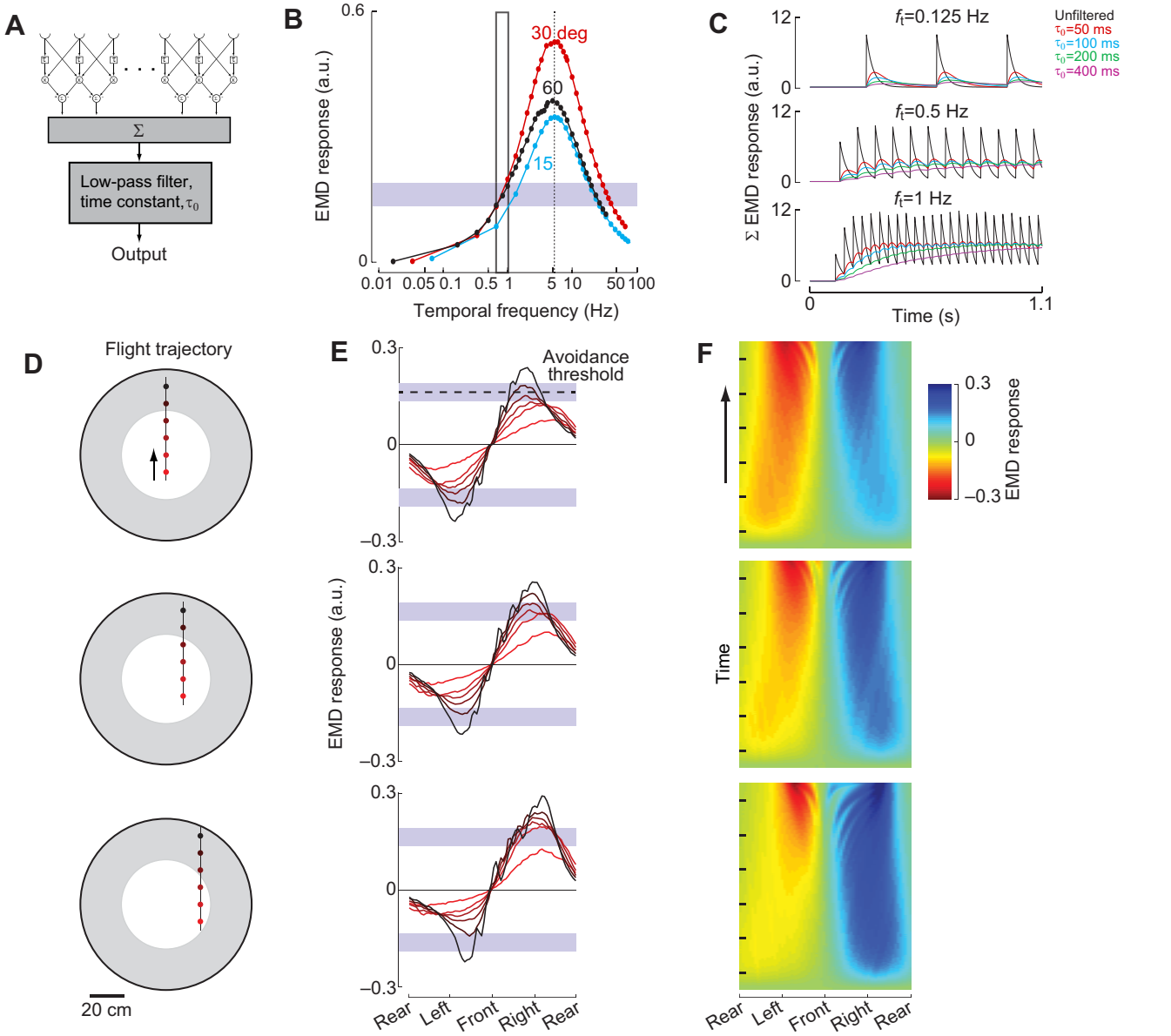

Fig. 6. A simulation of fly motion vision supports the relevance of tethered flight speed-dependent inversion to free flight results. (A) A schematic diagram for the simulated visual system, corresponding to the equatorial band of each eye with 36 ommatidia at the input. An array of HR EMDs followed by integration and filtering is used to model the fly visual system. After all EMD outputs are summed, a first-order low-pass filter (time constant τ_o) is applied. This time constant models the compounded delays and filtering that are thought to occur between motion detection and motor output. (B) The response curve for a single EMD unit with a time constant τ selected to capture the temporal frequency optimum of the *Drosophila* expansion-avoidance response, plotted against temporal frequency on a log scale. The EMD response depends on the spatial and temporal frequency of the patterns. Each point shows the result of the mean EMD output in response to stimulation with square-wave intensity gratings of the three spatial periods used in the experiments of Fig. 4. The temporal frequency optima of these curves coincide at the theoretically predicted value (for τ=30 ms) indicated by the vertical dashed line. The vertical bar outlines the 2/3–1 Hz band, in which the critical value for the speed-dependent inversion resides. (C) To facilitate a direct comparison with the results shown in Fig. 2A, the same pattern (30 deg square-wave with grayscale smoothing at the edges) was rotated (or expanded in front of the fly) at f_t=0.125, 0.5 and 1 Hz (corresponding to 3, 12 and 24 frames s^{-1}). The black traces show the summed EMD response (in arbitrary units), and the superimposed traces represented the EMD response once filtered by the first-order low-pass filter with the specified time constant. A value of τ_o=200 ms provides a qualitative agreement with the open-loop response data and is used in further simulations. The virtual flight simulations are modeled after free-flight behavior described in Tammero and Dickinson (Tammero and Dickinson, 2002). (D) Overhead view of the simulated environment in which the virtual fly is translated along straight flight trajectories within a 1 m diameter arena covered with a randomized checkerboard pattern (wall texture not shown). The arrow indicates the direction of motion and serves as a 1 s scale bar. The gray ring indicates the zone where visual motion is too high as flies are not likely to fly near the wall. The inner boundary of the gray ring indicates the distance from the center of the arena by which 75% of collision-avoidance saccades take place [based on data from Tammero and Dickinson (Tammero and Dickinson, 2002)]. The mean EMD array response is plotted at each position on the retina (E), while the simulated fly is at the position along the trajectory indicated by the matching color. The sign convention used is that clockwise (as viewed from above) motion is positive, such that progressive (front-to-back) motion on the right eye is positive and on the left eye is negative. The violet horizontal bars indicate the magnitude of the EMD response that corresponds to the response at the critical range for the speed-dependent behavior from B. A remarkable correspondence exists between the locations where flies tend not to fly (the gray zone in D) and local components of the EMD response that are at the top or above the violet band, suggestive of an 'avoidance threshold'. (F) The continuous version of the simulation results show the EMD response at each position on the retina for the duration of the flight, where pseudocolor represents magnitude. The tick marks denote the discrete locations at which the simulation results are shown in D and E.

frequencies than we could experimentally test) is shown in Fig. 6B. These curves show the averaged response of a single simulated EMD to open-loop advances of the grating patterns. Because the three patterns have different spatial periods, the angular velocity of the patterns was selected to yield the same temporal frequency. The curves show the expected shape of the HR EMD response; for increasing temporal frequencies there is a monotonically increasing response that peaks at the temporal frequency optimum (TFO) beyond which increasing the temporal frequency of the stimuli yields a decreasing response. Because the expansion-avoidance behavior (Fig. 4B) resembles an HR EMD response with a broad peak between 2 and 10 Hz, we tuned the EMD simulation with a time constant that would coincide with the middle of this range. A time constant τ=30 ms analytically yields a TFO of 5.3 Hz, and indeed the three response curves all peak at the predicted value, which is indicated by the dashed vertical black line. The vertical bar is added to outline the ⅔–1 Hz band, the temporal frequency range that is relevant for the critical value of the expansion response inversion (as a consensus value for the open loop results in Fig. 2 and the closed loop results of Fig. 4 – responses to expansion below this range are dominated by expansion attraction, whereas responses to stimuli above this range are dominated by orientation towards contraction). The horizontal violet band is added to emphasize the magnitude of the EMD response (in arbitrary units) to stimuli that are within this temporal frequency range (for λ=30 deg and λ=60 deg), and will be used to interpret free flight simulations to follow. Consistent with previous experimental results (Buchner, 1976), the spatial frequency dependence reveals a tuning whereby the response to the λ=30 deg pattern is closest to the spatial frequency optimum, and thus yields a larger EMD response at each temporal frequency. The response to λ=15 deg and λ=60 deg gratings are reduced but for different reasons. The λ=15 deg stimulus is attenuated by the low-pass optical filtering, whereas the contrast difference between the two ommatidia seeing the λ=60 deg pattern is usually small, minimizing the temporal coincidence in the motion detector.

We then used the fine structure of the open-loop data (Fig. 2) to motivate a simple model for the sensorimotor processing that occurs between the early visual system and the steering responses we measured. A previously proposed model for the optomotor response of flies consists of an HR EMD array, whose outputs are spatially integrated and then temporally low-pass filtered (Borst and Bahde, 1987; Warzecha and Egelhaaf, 1996). Warzecha and Egelhaaf (Warzecha and Egelhaaf, 1996) simulated such a system (with a first-order low-pass filter, time constant of 750 ms) to model the syndirectional optomotor control system of a blowfly. The low-pass filter is a black-box model for the delays and 'smoothing' that occur between the motion processing pathways and motor output, and was implemented in our simulation (shown for one eye, Fig. 6A).

To select the time constant for sensorimotor integration in our model, we made use of the time series data of Fig. 2A as a comparison for the simulated responses of Fig. 6C. The turning responses to slow expansion stimuli exhibit a prominent 'ripple' that is phase locked to the discrete advances of the pattern. This ripple is seen in the mean response to 0.125 Hz expansion (3 frames s^{-1}) and is also present in the responses to the 0.25 and 0.5 Hz expansion, but is virtually absent in the 1 Hz expansion responses. The identical pattern used in the experiment of Fig. 2 was simulated at the slower temporal frequencies used in Fig. 2. The summed EMD responses are shown in black, as are low-pass filtered versions of these responses (for visuomotor time constants 50, 100, 200 and 400 ms, shown color coded). The results of filtering with τ_o=200 ms provided a qualitative agreement with the open-loop data summarized above; there is a prominent ripple in the responses to the expansion at temporal frequencies of 0.125, 0.25 (not shown) and 0.5 Hz, which is largely attenuated in the response to f_t=1 Hz expansion.

The most appropriate free-flight data collected under controlled visual conditions that can serve as a 'ground truth' for the simulation results is presented by Tammero and Dickinson (Tammero and Dickinson, 2002), with similar experiments performed by Stewart and co-workers (Stewart et al., 2010). In the Tammero and Dickinson (Tammero and Dickinson, 2002) study, flies were tracked flying within a 1 m diameter cylinder, while the walls of the environment were covered with a randomized checkerboard pattern (each square of the checkerboard covered a 5 deg×5 deg patch when viewed from the center and was either black or white with 50% probability). In this environment, flies fly in nearly straight paths that are interspersed with rapid body saccades. In the simulation, the virtual fly was translated across the 1 m circular arena at 23 cm s^{-1} along one of three different straight paths: one directly down the midline of the arena and two lateral trajectories spaced 10 and 20 cm to the side of the midline (virtual flight paths shown in Fig. 6D). This flight velocity was the mean speed during flight in the textured background from fig. 5 of Tammero and Dickinson (Tammero and Dickinson, 2002). The fly's view of the arena was obtained using the procedure outlined in the Materials and methods. Initial simulation attempts [not shown, but see Reiser (Reiser, 2006)] using purely geometric estimates of visual motion contained significant overestimates of optic flow and were not suitable for comparison to our experimental results. The discrepancy indicates that it is critical to account for the temporal and spatial low-pass filtering characteristics of the fly eye by using the ommatidial sampling and HR EMD simulation.

The simulation results are shown in Fig. 6E, in which each curve is color coded to match the corresponding location along the trajectories of Fig. 6D. The EMD responses around the simulated retina were obtained as the mean responses of 500 runs along each trajectory, where in each case the relative orientation of the fly and the pattern on the wall were randomized. We show an average response because the results from individual simulations have the same general shape, but with large deviations that are dependent on the locations of specific high-contrast edges that differ across simulations. The results are shown without spatial integration so that the responses at all retinal positions can be seen (each EMD unit contributes one point to the curves), but the individual values were filtered with the visuomotor delay filter for better comparison with behavioral data. Fig. 6F shows the complete simulation with the local responses at all points in time shown using pseudo-color to indicate EMD magnitude.

To facilitate the comparison between the simulated open-loop tethered flight arena responses of the EMD and the EMD responses during the simulated free flight experiments, we indicate the magnitude of EMD responses (horizontal violet bars, Fig. 6E) to square-wave intensity pattern motion in the range of ⅔–1 Hz (the limits of this range were obtained by averaging the very similar response magnitudes to the λ=30 deg and λ=60 deg square-wave patterns in Fig. 6B). We again used data from Tammero and Dickinson (Tammero and Dickinson, 2002) to derive a distribution of saccade locations. The inner circle of the gray torus in each arena overview diagram (Fig. 6D, in gray) indicates the distance from the center of the arena by which 75% of all saccades take place [26.1 cm; determined by forming the cumulative probability distribution of saccade location from fig. 6 of Tammero and Dickinson (Tammero and Dickinson, 2002)]. For a fly flying through the center of the arena towards the wall, this zone represents the region in which the

visual cues are apparently too strong to sustain typical forward flight, as the majority of flies tend to saccade – in anticipation of a collision – before entering this zone.

The simulated responses capture many of the expected features of motion perceived during flight along these paths. All of the EMD responses show a frontal FOE, a point at which the motion response is zero. The FOE is always centered on the eye, even when the fly flies closer to one side of the arena, which is consistent with forward flight in the absence of body rotations or sideslip. These simulated responses show a reduction in the local motion response measured towards the rear of each eye, but there is no actual FOC point where EMD output is zero because this simulated visual system has a blind spot in the rear. As a fly approaches the wall from the center of the arena (top row), the EMD response increases and the slope of the curves at retinal position directly in front increases. The two trajectories in which the fly flies closer to one side of the arena show a marked asymmetry such that the eye that images the nearest wall produces the highest local EMD response at each location along the trajectory. Finally, a comparison of the EMD response with the violet band marking the critical value for the expansion inversion behavior shows a remarkable degree of correspondence between the locations where flies tend not to fly (because they saccade to avoid imminent collisions in response to excessive levels of visual motion) and local components of the EMD response that are at the top or above the violet band, which we term the 'avoidance threshold'. The emerging model that balances forward flight with collision-avoidance is simple: (1) forward flight is maintained by orienting towards a frontal FOE when collisions are unlikely and visual motion is low (consistent with the requirement for the frontal visual field for slow motion FOE attraction in Fig. 5), and (2) collision-avoidance is initiated when the integrated EMD response within even small parts of the lateral eye regions exceeds this avoidance threshold. We note that this model does not require an explicit estimate of either distance to the wall or the speed of visual motion but only the magnitude and spatial structure of the EMD response. Moreover, it predicts that the animals should tolerate some left–right asymmetry in the EMD response from both eyes, which is in contrast to the classical optomotor equilibrium model (Götz, 1968) but is consistent with free flight results, where the animals rarely fly down the center of the arena (Tammero and Dickinson, 2002; Stewart et al., 2010). Another prediction of the model is that free-flight collision-avoidance is not initiated by expansion *per se* but rather by only the magnitude and location of the progressive (front-to-back) component of the visual motion. An explicit test of this prediction will require future studies.

DISCUSSION

The open- and closed-loop experiments we conducted demonstrate that the magnitude and valence of the visual expansion response of *Drosophila* depends critically on stimulus strength. At low temporal frequency, flies exhibit an attraction to expansion patterns, which transforms to an avoidance at higher speeds. However, in open-loop experiments, flies with their heads glued to the thorax did not exhibit an attraction to expanding patterns at low temporal frequency (Fig. 1), whereas those with heads that were free did (Fig. 2). The inversion of the expansion-avoidance reflex with stimulus strength has a clear manifestation under closed-loop conditions, with flies actively orienting towards the FOE at low temporal frequency and preferring the FOC at high temporal frequency (Figs 3, 4). This tuning was not dependent on the spatial frequency of the pattern, suggesting that these behaviors are downstream of HR EMDs (Fig. 4). The dynamics of closed-loop FOE orientation are not qualitatively different from those during FOC orientation (Fig. 3), although the best conditions for FOC fixation are more attractive to the animals than the best conditions for expansion (Fig. 4). The change in the response direction with temporal frequency does not require that the motion stimulus be presented directly in front and behind the fly. Animals in which the stimulus was masked within a 60 deg sector in front and behind still exhibited FOE fixation at low temporal frequency and the switch to FOC fixation at high temporal frequency (Fig. 5). This switch was, however, not present when 120 deg sectors masked the front and rear stimulus regions, suggesting that expansion avoidance (and thus FOC fixation) requires the presence of information in the front visual field (Fig. 5B). Finally, a simple model based on HR EMDs shows that the reflex inversion we identified can explain the spatial distribution of collision-avoidance saccades when flies fly freely within an open circular arena (Fig. 6). Collectively, the results provide a new picture of how flies balance the need for stable forward flight with the avoidance of obstacles. In particular, these visual motor reflexes may represent a clutter-avoidance strategy in which the expanding flow patterns generated by distant objects (which is relatively gentle due to the inverse relationship between object distance and optic flow) stabilize forward flight, whereas the strength and spatial arrangement of optic flow cues generated by near objects elicit collision avoidance.

What does the discrepancy between head-fixed and head-free results suggest about the role of head motion?

The difference between the open-loop turning responses of head-free and head-fixed flies was an unexpected result. This is especially true in light of a recent detailed comparison of the responses of head-fixed and head-free flies in an identical experimental apparatus that found very few differences in the behavior of flies subjected to moving gratings presented unilaterally to one eye or binocularly (Duistermars et al., 2012). To our knowledge, the results reported in the present study are the first examples of significant behavioral differences caused by fixing the head of a tethered *Drosophila*. Head motion not only changes the visual stimuli perceived by the fly, it also engages additional reflex pathways involving halteres, neck mechanoreceptors and the neck motor system (Sandeman and Markl, 1980; Hengstenberg, 1991b), all of which are presumably disabled in head-glued flies. At present, however, we can offer no sensible explanation for why the presence of such pathways is required for flies to exhibit the inversion of the expansion-avoidance reflex that we measured. One possibility is that the head motion simply rotates the location on the retina at which the foci of the pattern occur. To test this possibility, we performed some simple observational studies with a camera focused on the heads of tethered (head-free) flies facing expanding stimuli with both low and high rates of expansion. During most flight bouts the head motion in flight generally consists of small, rapid movements, as well as large head motions that typically accompany large turns. As expected from prior studies (Hengstenberg, 1991a; Zanker et al., 1991; van Hateren and Schilstra, 1999), we observed a strong coordination between head yaw and wing motion, i.e. the head turned in the same direction of an intended turn. In order for the position of the FOE to cross the midline the head must rotate by more than the angular distance of the FOE from the midline. This is unlikely because the orientation towards the FOE exists for FOE position as great as 60 deg or more from the midline, and the head of *Drosophila* is unable to rotate by this amount due to morphological constraints [head turns of up to 25 deg, but not larger, were measured in the recent study by Duistermars et al. (Duistermars et al., 2012)]. In addition, it is not

at all clear why head motion would alter the visual experience of a fly during slow expansion and not during faster expansion.

The head orientation of the fixed-head flies may partially account for the discrepancy. As a tethered fly begins to fly, the head pitches forward considerably and remains in this position throughout flight. The head gluing procedure typically employed in arena experiments fixes the head in the position that would considerably alter the regions of the eye that perceive the expansion stimuli. Because the head is fixed at an increased, nose-up pitch angle, the direction of expanding motion, which will be perceived as roughly parallel to the eyes of a head-free fly, will contain a significant component of upwards motion in a head-fixed fly. It is possible that the system mediating the expansion orientation response is inhibited by this upward motion, which has been shown to initiate a 'thrust' response (Götz, 1968; Götz and Wandel, 1984).

A final possibility is that the dynamics of temporal processing in the early visual system may also account for this difference. The synchronous delivery of infrequent motion events that comprise the slow stimuli we deliver, may be treated very differently by the early visual system when the head of a fly is fixed. When the visual system of the animal is stabilized, slow speed expansion stimuli may rapidly be adapted away by the high pass filtering in the photoreceptor and lamina networks (Laughlin and Hardie, 1978; Harris and O'Carroll, 2002; Borst et al., 2003). However, the minimal amount of jitter introduced by head movements would disrupt this synchronicity, and thus produce a markedly different signal for subsequent motion stages.

Do the properties of fly motion detection predict the speed-dependent inversion?

One tantalizing suggestion is that the bell-shaped response curve predicted by HR EMDs and observed in a wide variety of behavioral and electrophysiological studies (Reichardt, 1961; Hausen and Wehrhahn, 1989) in some way explains the speed dependence of the expansion response. There is, however, little evidence to support this idea. One difficulty is that the TFO of *Drosophila* is now believed to be at least 5 Hz [supported by Fig. 4 in this study, as well as in prior work (Duistermars et al., 2007; Fry et al., 2009)], but the critical value governing the speed-dependent inversion is not more than 1 Hz. Furthermore, the fact that the monotonicity of the motion detector response (increasing temporal frequency yielding increasing EMD response) reverses beyond the TFO can only explain changes in response amplitude, not a sign inversion. In addition, because in all of the experiments both eyes receive motion at the same temporal frequency, the decay in motion responses above the TFO cannot explain the inversion of the expansion-avoidance response. As a final consideration, we note that the HR EMD responses we simulated in free flight do not show any evidence for a sign inversion. Rather as the fly proceeds from weak motion to strong motion (Fig. 6E, top row), the profile of the EMD response around the eye is maintained and the amplitude gradually increases as a fly crosses the arena. One conclusion of this study is that it is far more likely that much of navigation occurs at lower values of image motion (on the monotonically increasing side of the EMD curve), whereas at higher speeds the strong, expansion-avoidance responses dominate the flies' behavior.

Closed-loop results with modified expansion avoidance stimuli

Animals in which front and rear sectors of 60 deg were masked still exhibited the inversion of the expansion-avoidance reflex with temporal frequency, although (expectedly) the fixation was not nearly as precise. This experiment, which approximates the flow experienced when flying down a tunnel, was designed to test whether the phenomenon was an artifact of a circular arena display. Restricting the field of view even further by extending the front and rear masks to 120 deg yielded an unexpected result in which the orientation towards a FOE was not further reduced, and rather appeared 'normal', but animals exhibited diminished FOC fixation, especially at the higher temporal frequencies. Basically, when the stimulus motion was restricted to 60 deg sector to the left and right, flies exhibited no expansion avoidance, but could steer towards expansion if the temporal frequency was sufficiently low. Thus the attraction to expansion at lower rates of image motion can be maintained without any information from the frontal region of the eye. This finding suggests that the FOE attraction documented here in tethered flight for flies may be analogous to the centering response in bees, which is also thought to depend on motion perceived at 90 deg to the direction of flight (Srinivasan et al., 1991).

Is there evidence of expansion avoidance inversion in free flight?

One challenge to our understanding of the visual control of flight is the non-monotonic response properties of the HR motion detectors, featuring a sensitivity peak at the temporal frequency optimum and attenuated responses above and below that speed. There is no consensus about what part of the HR input–output curve is most typically experienced by a fly during relevant behaviors. The model put forward by Götz (Götz, 1975) suggested that the entire range is relevant. Another suggestion is that the shape of the HR response curve provides flight stability (Warzecha and Egelhaaf, 1996), because the response to visual motion during very rapid turns is attenuated. This claim is supported by results in *Drosophila*, where the visual system has little influence during rapid body saccades (Bender and Dickinson, 2006).

The expansion attraction behavior that we observe in tethered flight relates to visual control of flight at the other extreme of possible visual motion inputs, where stability is not an issue. Because it is very unlikely that the behavioral inversion of expansion avoidance is caused by the shape of the HR EMD response curve (see above), the findings of the present study suggest that much, if not most of navigation behaviors operate on the monotonically increasing portion of the HR EMD response curve corresponding to lower temporal frequencies. This idea is strengthened by the new results suggesting that the TFO of *Drosophila* motion detection is higher than previously thought (see above). It is noteworthy that the largest EMD responses during the simulated flight of Fig. 6E only reach about half of the peak response of the EMD obtained in the simulations of the tethered flight open loop arena experiments of Fig. 6B. This is further evidence suggesting that during much of *Drosophila* behavior the motion-detecting system is operating at output levels well below those corresponding to stimulation at the TFO. While *Drosophila* are clearly capable of flight speeds above 23 cm s^{-1} (David, 1978; Budick and Dickinson, 2006), these flight speeds are reduced in the presence of a highly textured visual surround (Tammero and Dickinson, 2002; Stewart et al., 2010). Therefore, it is unlikely that during faster flight a fly would encounter visual motion that is considerably stronger than in the simulations of Fig. 6D–F.

The peak magnitude of EMD responses during the simulated translatory flight of Fig. 6 show strong correspondence to the magnitude of EMD responses simulated with the stimuli that elicit the expansion-attraction response in *Drosophila*. The peak responses of the EMD array during flight segments that are within the strong

stimulus (super-threshold) zone (gray ring in Fig. 6D) exceed the range that corresponds to simulated open-loop responses for stimuli within the critical value of the expansion response (depicted by the violet bands in Fig. 6E). This finding suggests that the expansion-attraction response is required to explain the free flight data (Tammero and Dickinson, 2002; Stewart et al., 2010), and probably accounts for the weak centering tendency observed between saccades, where flies were found to turn slightly away from the closer side of the arena [fig. 8 of Tammero and Dickinson (Tammero and Dickinson, 2002)]. An inspection of the EMD responses in Fig. 6E suggests that the proposed sensitivity of the expansion attraction response to lateral retinal positions (see Fig. 5) is plainly sensible because very little motion is seen by frontal eye regions during forward flight, whereas the lateral regions exhibit the asymmetry that occurs during non-centered flight. The simulated results may explain why even more centering was not observed in the free flight data of Tammero and Dickinson (Tammero and Dickinson, 2002). If the centering behavior is indeed a response to left–right asymmetry, then the visual conditions in the flight arena were such that only large deviations from a centered trajectory would result in the asymmetry of retinal motion required to produce a strong centering response. Other experiments (not shown) suggest that flies tolerate a small amount of motion asymmetry (tested with a 1:2 ratio) while orienting towards a FOE. Furthermore, when flies were flown in a cylindrical environment lined with horizontal stripes, the flight trajectories are curved, faster and much closer to the walls (Frye et al., 2003). It is likely that in the absence of strong horizontal motion cues the saccadic response is suppressed, while the centering response dominates flight. These observations suggest that the centering response and the saccadic system may be separate, parallel systems with distinct spatial and temporal tunings. As a final note about the critical value of the speed-dependent inversion, the recent results with freely flying *Drosophila* in a novel 'virtual open-loop' experiment (Fry et al., 2009) show that the preferred flight speed of *Drosophila* in a tunnel lined with a sine wave grating corresponds to a laterally perceived temporal frequency of ~1 Hz. This result provides a methodologically independent corroboration of the behavioral relevance of the described inversion that governs the transition from expansion attraction during forward flight to expansion avoidance. One exciting implication of this newly established role for slow motion visual stimuli is that this stimulus regime may be ideally suited for the limited temporal dynamics that can be extracted from calcium imaging in the fly visual system (Reiff et al., 2010; Clark et al., 2011).

LIST OF ABBREVIATIONS

ΔWBA	difference between left and right wing beat amplitudes
FDR	false discovery rate
FOC	focus of contraction
FOE	focus of expansion
HR EMD	Hassenstein–Reichardt elementary motion detector
LED	light emitting diode
TFO	temporal frequency optimum

ACKNOWLEDGEMENTS

We thank Dr Mark Frye and members of the Dickinson lab for constructive feedback throughout the development of this project.

FUNDING

This work was supported by the Institute for Collaborative Biotechnologies through grant DAAD 19-03-D-0004 from the US Army Research Office, by the National Science Foundation (NSF) through award 0623527 to M.H.D. and by the Center for Neuromorphic Systems Engineering (CNSE) Engineering Research Center at Caltech through NSF award EEC-9402726.

REFERENCES

Bender, J. A. and Dickinson, M. H. (2006). A comparison of visual and haltere-mediated feedback in the control of body saccades in *Drosophila melanogaster*. *J. Exp. Biol.* **209**, 4597-4606.
Benjamini, Y. and Hochberg, Y. (1995). Controlling the false discovery rate – a practical and powerful approach to multiple testing. *J. Roy. Stat. Soc. B Met.* **57**, 289-300.
Borst, A. and Bahde, S. (1987). Comparison between the movement detection systems underlying the optomotor and the landing response in the housefly. *Biol. Cybern.* **56**, 217-224.
Borst, A. and Egelhaaf, M. (1989). Principles of visual motion detection. *Trends Neurosci.* **12**, 297-306.
Borst, A., Reisenman, C. and Haag, J. (2003). Adaptation of response transients in fly motion vision. II: Model studies. *Vision Res.* **43**, 1311-1324.
Büchner, E. (1974). *Bewegungsperzeption in einem visuellen System mit gerastertem Eingang*. PhD thesis, University of Tubingen, Germany.
Buchner, E. (1976). Elementary movement detectors in an insect visual system. *Biol. Cybern.* **24**, 85-101.
Buchner, E. (1984). Behavioural analysis of spatial vision in insects. In *Photoreception and Vision in Invertebrates* (ed. M. A. Ali), pp. 561-621. New York: Plenum.
Budick, S. A. and Dickinson, M. H. (2006). Free-flight responses of *Drosophila melanogaster* to attractive odors. *J. Exp. Biol.* **209**, 3001-3017.
Budick, S. A., Reiser, M. B. and Dickinson, M. H. (2007). The role of visual and mechanosensory cues in structuring forward flight in *Drosophila melanogaster*. *J. Exp. Biol.* **210**, 4092-4103.
Burton, B. G. and Laughlin, S. B. (2003). Neural images of pursuit targets in the photoreceptor arrays of male and female houseflies *Musca domestica*. *J. Exp. Biol.* **206**, 3963-3977.
Clark, D. A., Bursztyn, L., Horowitz, M. A., Schnitzer, M. J. and Clandinin, T. R. (2011). Defining the computational structure of the motion detector in *Drosophila*. *Neuron* **70**, 1165-1177.
David, C. T. (1978). The relationship between body angle and flight speed in free-flying *Drosophila*. *Physiol. Entomol.* **3**, 191-195.
David, C. T. (1982). Compensation for height in the control of groundspeed by *Drosophila* in a new, 'barber's pole' wind tunnel. *J. Comp. Physiol. A* **147**, 485-493.
Duistermars, B. J., Chow, D. M., Condro, M. and Frye, M. A. (2007). The spatial, temporal and contrast properties of expansion and rotation flight optomotor responses in *Drosophila*. *J. Exp. Biol.* **210**, 3218-3227.
Duistermars, B. J., Care, R. A. and Frye, M. A. (2012). Binocular interactions underlying the classic optomotor responses of flying flies. *Frontiers* **6**, 6.
Franceschini, N., Ruffier, F. and Serres, J. (2007). A bio-inspired flying robot sheds light on insect piloting abilities. *Curr. Biol.* **17**, 329-335.
Fry, S. N., Rohrseitz, N., Straw, A. D. and Dickinson, M. H. (2009). Visual control of flight speed in *Drosophila melanogaster*. *J. Exp. Biol.* **212**, 1120-1130.
Frye, M. A., Tarsitano, M. and Dickinson, M. H. (2003). Odor localization requires visual feedback during free flight in *Drosophila melanogaster*. *J. Exp. Biol.* **206**, 843-855.
Gibson, J. J. (1950). *The Perception of the Visual World*. Oxford: Houghton Mifflin.
Götz, K. G. (1968). Flight control in *Drosophila* by visual perception of motion. *Kybernetik* **4**, 199-208.
Götz, K. G. (1975). Optomotor equilibrium of *Drosophila* navigation system. *J. Comp. Physiol. A* **99**, 187-210.
Götz, K. G. (1987). Course-control, metabolism and wing interference during ultralong tethered flight in *Drosophila melanogaster*. *J. Exp. Biol.* **128**, 35-46.
Götz, K. G. and Wandel, U. (1984). Optomotor control of the force of flight in *Drosophila* and *Musca*. *Biol. Cybern.* **51**, 135-139.
Harris, R. A. and O'Carroll, D. C. (2002). Afterimages in fly motion vision. *Vision Res.* **42**, 1701-1714.
Hassenstein, V. B. and Reichardt, W. (1956). Systemtheoretische Analyse der Zeit-, Reihenfolgen und Vorzeichenauswertung bei der Bewegungsperzeption des Russelkafers Chlorophanus. *Z. Naturforschg.* **11b**, 513-524.
Hatsopoulos, N., Gabbiani, F. and Laurent, G. (1995). Elementary computation of object approach by wide-field visual neuron. *Science* **270**, 1000-1003.
Hausen, K. and Wehrhahn, C. (1989). Neural circuits mediating visual flight control in flies. I. Quantitative comparison of neural and behavioral response characteristics. *J. Neurosci.* **9**, 3828-3836.
Heisenberg, M. and Wolf, R. (1984). *Vision in Drosophila: Genetics of Microbehavior*. Berlin, Germany: Springer-Verlag.
Helmholtz, H. and Southall, J. (1925). Treatise on physiological optics. III. *The Perceptions of Vision*. New York: Optical Society of America.
Hengstenberg, R. (1991a). Head posture, body posture and gaze movements in the resting and flying fruitfly *Drosophila*. *Synapse* **1991**, 273.
Hengstenberg, R. (1991b). Gaze control in the blowfly *Calliphora*: a multisensory, two-stage integration process. *Semin. Neurosci.* **3**, 19-29.
Kung, C. (1971). Genic mutants with altered system of excitation in *Paramecium aurelia*. II. Mutagenesis, screening and genetic analysis of the mutants. *Genetics* **69**, 29-45.
Lappe, M., Bremmer, F. and van den Berg, A. V. (1999). Perception of self-motion from visual flow. *Trends Cogn. Sci.* **3**, 329-336.
Laughlin, S. B. and Hardie, R. C. (1978). Common strategies for light adaptation in the peripheral visual systems of fly and dragonfly. *J. Comp. Physiol.* **128**, 319-340.
Lehmann, F. O. and Dickinson, M. H. (1997). The changes in power requirements and muscle efficiency during elevated force production in the fruit fly *Drosophila melanogaster*. *J. Exp. Biol.* **200**, 1133-1143.
Maimon, G., Straw, A. D. and Dickinson, M. H. (2008). A simple vision-based algorithm for decision making in flying *Drosophila*. *Curr. Biol.* **18**, 464-470.
Nelson, M. E. and MacIver, M. A. (2006). Sensory acquisition in active sensing systems. *J. Comp. Physiol. A* **192**, 573-586.

Reichardt, W. (1961). Autocorrelation, a principle for the evaluation of sensory information by the central nervous system. In *Sensory Communication* (ed. W. A. Rosenblith), pp. 303-317. Cambridge, MA: MIT Press.
Reiff, D. F., Plett, J., Mank, M., Griesbeck, O. and Borst, A. (2010). Visualizing retinotopic half-wave rectified input to the motion detection circuitry of *Drosophila*. *Nat. Neurosci.* **13**, 973-978.
Reiser, M. B. (2006). Visually mediated control of flight in *Drosophila*: not lost in translation. PhD thesis, California Institute of Technology, Pasadena, CA, USA.
Reiser, M. B. and Dickinson, M. H. (2008). A modular display system for insect behavioral neuroscience. *J. Neurosci. Methods* **167**, 127-139.
Reiser, M. B. and Dickinson, M. H. (2010). *Drosophila* fly straight by fixating objects in the face of expanding optic flow. *J. Exp. Biol.* **213**, 1771-1781.
Robertson, R. M. and Reye, D. N. (1992). Wing movements associated with collision avoidance manoeuvres during flight in the locust *Locusta migratoria*. *J. Exp. Biol.* **163**, 231-258.
Sandeman, D. C. and Markl, H. (1980). Head movements in flies (*Calliphora*) produced by deflexion of the halteres. *J. Exp. Biol.* **85**, 43-60.
Snyder, A. W. (1979). Physics of vision in compound eyes. *Handb. Sens. Physiol.* **7**, 225-313.
Srinivasan, M. V., Lehrer, M., Kirchner, W. H. and Zhang, S. W. (1991). Range perception through apparent image speed in freely flying honeybees. *Vis. Neurosci.* **6**, 519-535.
Stewart, F. J., Baker, D. A. and Webb, B. (2010). A model of visual-olfactory integration for odour localisation in free-flying fruit flies. *J. Exp. Biol.* **213**, 1886-1900.
Tammero, L. F. and Dickinson, M. H. (2002). The influence of visual landscape on the free flight behavior of the fruit fly *Drosophila melanogaster*. *J. Exp. Biol.* **205**, 327-343.
Tammero, L. F., Frye, M. A. and Dickinson, M. H. (2004). Spatial organization of visuomotor reflexes in *Drosophila*. *J. Exp. Biol.* **207**, 113-122.
van Hateren, J. H. and Schilstra, C. (1999). Blowfly flight and optic flow. II. Head movements during flight. *J. Exp. Biol.* **202**, 1491-1500.
Wagner, H. (1982). Flow-field variables trigger landing in flies. *Nature* **297**, 147-148.
Wang, Y. and Frost, B. J. (1992). Time to collision is signalled by neurons in the nucleus rotundus of pigeons. *Nature* **356**, 236-238.
Warzecha, A. K. and Egelhaaf, M. (1996). Intrinsic properties of biological motion detectors prevent the optomotor control system from getting unstable. *Philos. Trans. R. Soc. B* **351**, 1579-1591.
Zanker, J. M., Egelhaaf, M. and Warzecha, A.-K. (1991). On the coordination of motor output during visual flight control of flies. *J. Comp. Physiol. A* **169**, 127-134.